

1 Dead zone or oasis in the open ocean? Zooplankton 2 distribution and migration in low-oxygen modewater 3 eddies

4
5 H. Hauss¹, S. Christiansen¹, F. Schütte¹, R. Kiko¹, M. Edvam Lima², E.
6 Rodrigues², J. Karstensen¹, C.R. Löscher^{1,3}, A. Körtzinger^{1,4} and B. Fiedler¹

7 [1]{GEOMAR Helmholtz Centre for Ocean Research Kiel, Düsternbrooker Weg 20, 24105
8 Kiel, Germany}

9 [2]{Instituto Nacional de Desenvolvimento das Pescas (INDP), Cova de Inglesa, Mindelo,
10 São Vicente, Cabo Verde}

11 [3]{Institute for General Microbiology, Kiel, Germany}

12 [4]{Christian Albrecht University Kiel, Kiel, Germany}

13
14 Correspondence to: H. Hauss (hhauss@geomar.de)

15 16 **Abstract**

17 The eastern tropical North Atlantic (ETNA) features a mesopelagic oxygen minimum zone
18 (OMZ) at approximately 300-600 m depth. Here, oxygen concentrations rarely fall below 40
19 $\mu\text{mol O}_2 \text{ kg}^{-1}$, but are expected to decline under future projections of global warming. The
20 recent discovery of mesoscale eddies that harbour a shallow suboxic ($<5 \mu\text{mol O}_2 \text{ kg}^{-1}$) OMZ
21 just below the mixed layer could serve to identify zooplankton groups that may be negatively
22 or positively affected by on-going ocean deoxygenation. In spring 2014, a detailed survey of a
23 suboxic anticyclonic modewater eddy (ACME) was carried out near the Cape Verde Ocean
24 Observatory (CVOO), combining acoustic and optical profiling methods with stratified
25 multinet hauls and hydrography. The multinet data revealed that the eddy was characterized
26 by an approximately 1.5-fold increase in total area-integrated zooplankton abundance. At
27 nighttime, when a large proportion of acoustic scatterers is ascending into the upper 150 m, a
28 drastic reduction in mean volume backscattering (S_v , shipboard ADCP, 75kHz) within the

29 shallow OMZ of the eddy was evident compared to the nighttime distribution outside the
30 eddy. Acoustic scatterers were avoiding the depth range between about 85 to 120 m, where
31 oxygen concentrations were lower than approximately $20 \mu\text{mol O}_2 \text{ kg}^{-1}$, indicating habitat
32 compression to the oxygenated surface layer. This observation is confirmed by time-series
33 observations of a moored ADCP (upward looking, 300kHz) during an ACME transit at the
34 CVOO mooring in 2010. Nevertheless, part of the diurnal vertical migration (DVM) from the
35 surface layer to the mesopelagic continued through the shallow OMZ. Based upon vertically
36 stratified multinet hauls, Underwater Vision Profiler (UVP5) and ADCP data, four strategies
37 have been identified to be followed by zooplankton in response to the eddy OMZ: i) shallow
38 OMZ avoidance and compression at the surface (e.g. most calanoid copepods, euphausiids),
39 ii) migration to the shallow OMZ core during daytime, but paying O_2 debt at the surface at
40 nighttime (e.g. siphonophores, *Oncaea* spp., eucalanoid copepods), iii) residing in the shallow
41 OMZ day and night (e.g. ostracods, polychaetes), and iv) DVM through the shallow OMZ
42 from deeper oxygenated depths to the surface and back. For strategy i), ii) and iv),
43 compression of the habitable volume in the surface may increase prey-predator encounter
44 rates, rendering zooplankton and micronekton more vulnerable to predation and potentially
45 making the eddy surface a foraging hotspot for higher trophic levels. With respect to long-
46 term effects of ocean deoxygenation, we expect avoidance of the mesopelagic OMZ to set in
47 if oxygen levels decline below approximately $20 \mu\text{mol O}_2 \text{ kg}^{-1}$. This may result in a positive
48 feedback on the OMZ oxygen consumption rates, since zooplankton and micronekton
49 respiration within the OMZ as well as active flux of dissolved and particulate organic matter
50 into the OMZ will decline.

51

52 **1 Introduction**

53 The habitat of pelagic marine organisms is vertically structured by several biotic and abiotic
54 factors, such as light, prey density, temperature, oxygen concentration and others. In the
55 eastern tropical North Atlantic (ETNA), a permanent oxygen minimum zone (OMZ) exists in
56 the mesopelagial. The core of this OMZ is centered at approximately 450 m, with the upper
57 and lower oxyclines at approximately 300 and 600 m depth (Karstensen et al., 2008). Oxygen
58 concentrations in this deep OMZ hardly fall below $40 \mu\text{mol O}_2 \text{ kg}^{-1}$ (Karstensen et al., 2008),
59 but are sufficiently low to exclude highly active top predators such as billfishes from the
60 OMZ (Prince et al., 2010, Stramma et al. 2012). In the eastern tropical South Atlantic, with its

61 more pronounced midwater OMZ, this layer may act as an effective barrier for some species
62 (e.g. Auel and Verheye, 2007; Teuber et al., 2013), but seems to be diurnally crossed by
63 others (Postel et al., 2007). Many zooplankton and nekton taxa perform diurnal vertical
64 migrations (DVMs), usually spending the daylight hours in the mesopelagic OMZ and
65 migrating into the productive surface layer at night. These taxa include for example
66 euphausiids (Tremblay et al., 2011), sergestid and penaeid shrimp (Andersen et al., 1997),
67 myctophid fishes (Kinzer and Schulz, 1985) as well as several large calanoid copepods (e.g.
68 *Pleuromamma* species, Teuber et al., 2013). As DVM is a survival mechanism to evade
69 predation, hindrance thereof could lead to substantial changes in ecosystem functioning. The
70 ETNA OMZ has been observed to intensify (i.e. decrease in core O₂ concentrations) and
71 vertically expand over the past decades and is predicted to further deoxygenate and expand
72 laterally (Stramma et al., 2008; Stramma et al., 2009) under future expectations of
73 anthropogenic global warming (Cocco et al., 2013).

74 Submesoscale and mesoscale eddies (which in the tropics/subtropics comprise diameters on
75 the order of 10¹ and 10² km, respectively) often represent hotspots (or “oases”) of biological
76 productivity in the otherwise oligotrophic open ocean (e.g. Menkes et al., 2002; McGillicuddy
77 et al., 2007; Godø et al., 2012), translating even up to top predators (Tew Kai and Marsac,
78 2010). Their basin-wide relevance for biogeochemical cycles is increasingly recognized (e.g.
79 Stramma et al., 2013). Numerous eddies spin off the productive Mauritanian and Senegalese
80 coast (between Cap Blanc and Cap Vert) throughout the year, with most anticyclones being
81 generated in summer/autumn and most cyclones in winter/spring (Schütte et al., 2015a). Both
82 eddy types propagate westward at about 4 to 5 km day⁻¹, passing the Cape Verde archipelago
83 north or south. They can be tracked by satellite altimetry for up to nine months (Schütte et al.
84 2016; Karstensen et al., 2015). While “normal” anticyclones are usually relatively warm and
85 unproductive (e.g. Palacios et al., 2006), both cyclonic and anticyclonic mode water eddies
86 (ACMEs) are characterized by a negative sea surface temperature (SST) and positive surface
87 chlorophyll-*a* (chl-*a*) anomaly (Goldthwait and Steinberg; 2008; McGillicuddy et al., 2007).
88 In particular, ACMEs were observed to exceed cyclones in terms of upwelled nutrients and
89 productivity in the subtropical Atlantic (McGillicuddy et al., 2007).

90 The recent discovery of mesoscale eddies (cyclones and ACMEs) with extremely low oxygen
91 concentrations just below the mixed layer (Karstensen et al., 2015) has changed our view of
92 current oxygen conditions in the ETNA. In that study, it had been observed that oxygen

93 values $<2 \mu\text{mol O}_2 \text{ kg}^{-1}$ can be found in the shallow oxygen minimum. The authors concluded
94 that the low oxygen concentrations were the result of isolation of the eddy core against
95 surrounding water (a result of the rotation of the eddy) paired with enhanced respiration (a
96 result of the high productivity and subsequent export and degradation of particulate organic
97 matter, Fischer et al., 2015), and introduced the term “dead-zone eddy” (Karstensen et al.
98 2015). The so far lowest oxygen concentrations in such an eddy ($<2 \mu\text{mol O}_2 \text{ kg}^{-1}$ at about
99 40 m depth) were observed in February 2010 at the Cape Verde Ocean Observatory (CVOO)
100 mooring. During the eddy passage across the mooring, an almost complete lack of acoustic
101 scatterers at depth below the oxygenated mixed layer was observed. The acoustic backscatter
102 signal received by the 300 kHz ADCP is largely created by organisms $> 5 \text{ mm}$ (thus missing a
103 substantial part of the mesozooplankton) and does not enable the discrimination of different
104 zooplankton groups.

105 Here, we characterize the ecology of zooplankton in response to the shallow OMZ within an
106 ACME that was identified, tracked and sampled in spring 2014. We used acoustic (shipboard
107 ADCP) and optical (Underwater Vision Profiler) profiling methods as well as vertically
108 stratified plankton net hauls to resolve the vertical and horizontal distribution of zooplankton.
109 Moreover, we used acoustic and oxygen time series data from the CVOO mooring of one
110 extreme low oxygen eddy observed in February 2010 (Karstensen et al. 2015, Fischer et al.
111 2015) to derive a more general picture about the zooplankton sensitivity to low oxygen
112 concentrations.

113

114 **2 Materials and Methods**

115 In order to characterize the ecology, biogeochemistry and physical processes associated with
116 low oxygen eddies in the tropical North Atlantic, a dedicated field experiment (“eddy hunt”)
117 north of the Cape Verde Archipelago was designed. In summer 2013, the identification and
118 tracking of candidate eddies was started by combining remotely sensed data and Argo float
119 profile data. In spring 2014, a candidate low oxygen eddy was identified and on-site sampling
120 with gliders and research vessels began, covering genomics, physics, and biogeochemistry
121 (see also Löscher et al. 2015, Schütte et al. 2016, Fiedler et al. 2016, , Karstensen et al. 2016;
122 this issue). Ship-based sampling (“site survey”) presented here was carried out on March 18th
123 and 19th, 2014 during the RV *Meteor* cruise M105. Two ADCP sections perpendicular to each

124 other, a CTD/UVP5 cast section, and five multinet hauls were conducted. To better
125 characterize the average distribution of zooplankton during “normal” conditions in the
126 investigation area (as compared to conditions within the eddy), we combined the single time
127 point observation at the CVOO time series station with previously collected data at the same
128 station. For the multinet data, we used three additional day/night casts (RV *Maria S. Merian*
129 cruise MSM22: Oct 25, 2012 and Nov 20, 2012; RV *Meteor* cruise M97: May 26, 2013). For
130 the UVP data, we used seven nighttime profiles (because the four eddy core stations were
131 obtained during nighttime only) from cruises M105, MSM22, M97 and M106 (April 19/20,
132 2014). All data are publically available in the PANGAEA database ([doi to be added](#)).

133 In order to evaluate in greater detail the critical oxygen concentrations that lead to avoidance
134 behaviour we used the mean volume backscatter (S_v) and oxygen time series data from the
135 CVOO mooring. Here, we focus on the spring 2010 period that covered the transit of an
136 extreme low oxygen eddy, with oxygen content $<2\mu\text{mol kg}^{-1}$ (Karstensen et al., 2015).

137 **2.1 ADCP**

138 Underway current measurements were performed during cruise M105 using two vessel
139 mounted Acoustic Doppler Current Profilers (vmADCP), a 75kHz RDI Ocean Surveyor
140 (OS75) and a 38kHz RDI Ocean Surveyor (OS38). Standard techniques (see Fischer et al.,
141 2003) were used for data post-processing. Depending on the region and sea state, the ranges
142 covered by the instruments are around 550 m for the OS75 and around 1000 m for the OS38.
143 To locate the eddy center from the observed velocities, two sections were conducted (Fig. 1).
144 The first was a southeast-to-northwest section through the estimated (by remote sensing) eddy
145 center. The second section was a perpendicular, northeast-to-southwest section through the
146 location of lowest cross-sectional current velocity of the first section. The lowest cross-
147 sectional velocity of the second section defines the eddy center.

148 The ADCP installed at the CVOO mooring site in 109 m water depth was an upward looking
149 300kHz Teledyne RDI workhorse instrument, recording data every 1.5 hours. It has a 4 beam
150 design in Janus configuration with 20° opening. Based on accompanying hydrographic and
151 pressure data each 4 m depth cell was allocated a discrete pressure/depth information as well
152 as a sound speed profile (harmonic mean).

153 For vessel-mounted as well as moored ADCP, the mean volume backscatter S_v (MacLennan
154 et al, 2002) was estimated for each beam and each depth cell by a recalculation of a simplified

155 sonar equation (Deimes 1999). From the vessel-mounted ADCPs, only the OS75 was used to
156 assess backscatter distribution. Because we were not attempting to estimate biomass, no
157 further calibration was applied. S_v from the four ADCP beams was averaged and matched to
158 the oxygen data. Only data from January 1, 2010 to March 14, 2010 were used for the
159 analysis to avoid the influence of seasonal changes in scatterer abundance. Data collected
160 from 11:00 to 18:00 UTC and from 22:00 to 07:00 UTC were considered daytime and
161 nighttime data, respectively. Apparent sunrise and sunset in the period of January to March
162 are around 08:00 and 19:30 UTC, respectively.

163 **2.2 CTD and UVP5**

164 Oxygen concentration was measured using a SBE CTD with two SBE 43 oxygen sensors. The
165 oxygen sensors were calibrated against 641 discrete oxygen samples measured by Winkler
166 titration during cruise M105. Inside the CTD-rosette, a UVP5 was mounted. This imaging
167 tool allows *in situ* quantification of particles $>60 \mu\text{m}$ and plankton $>500 \mu\text{m}$ with high vertical
168 resolution (Picheral et al., 2010). Thumbnails of all objects $> 500 \mu\text{m}$ were extracted using the
169 ImageJ-based ZooProcess macro set (Gorsky et al., 2010) and sorted automatically into 41
170 categories using Plankton Identifier (Gasparini, 2007). Experts validated the automated image
171 sorting. The observed volume of each image was 0.93 L and approximately ten images were
172 recorded per meter depth. The mean total sampling volume for the upper 600 m of the water
173 column was $6.34 (\pm 0.99) \text{ m}^3$. Volume-specific abundance was calculated in 5 m depth bins.

174 **2.3 Multinet**

175 Zooplankton samples were collected with a Hydrobios multinet Midi (0.25 m^2 mouth
176 opening, 5 nets, 200 μm mesh, equipped with flowmeters) hauled vertically from the
177 maximum depth to the surface at 1 m s^{-1} .

178 A full “day/night” multinet station was conducted well outside of the eddy at 17.3474° N and
179 24.1498° W at the CVOO site, where a set of physical and biogeochemical variables are
180 measured on a monthly basis. For this reason, CVOO standard depths were used in this
181 multinet haul (800-600-300-200-100-0 m) as it also served the time series observations. As
182 the NW-ward eddy transect was conducted during daytime, the “eddy core day” multinet haul
183 was collected on this transect (12:40 UTC) and the “eddy core night” haul was collected at
184 02:10 UTC during the second transect (for classification of stations, see hydrography results

185 section), at the location of the CTD profile with the lowest O₂ concentration. Thus, the “eddy
186 core day” haul is approximately 14 km away from the eddy center (Fig.1). Depth intervals
187 (600-300-200-120-85-0 m) were chosen according to the O₂ profile. When leaving the eddy, a
188 second “day” haul was collected at the margin of the eddy, approximately 26 km from the
189 eddy center, using the depth intervals from the eddy core station. Zooplankton samples were
190 fixed in 100 mL Kautex® jars in 4% borax-buffered formaldehyde in seawater solution.

191 Zooplankton samples were analysed using a modification of the ZooScan Method (Gorsky et
192 al., 2010), employing an off-the-shelf flatbed scanner (Epson Perfection V750 Pro) and a scan
193 chamber constructed of a 21 cm x 29.7 cm (DIN-A4) size glass plate with a plastic frame.
194 Scans were 8bit grayscale, 2400 dpi images (Tagged image file format; *.tif). The scan area
195 was partitioned into two halves (i.e., two images per scanned frame) to reduce the size of the
196 individual images and facilitate the processing by ZooProcess/ImageJ. Samples were size-
197 fractionated by sieving into three fractions (<500 µm, 500-1000 µm, >1000 µm) and split
198 using a Motoda plankton splitter if necessary. The >1000 µm fraction was scanned
199 completely, whereas fractions comprising not more than approximately 1000 objects were
200 scanned for the two other fractions. “Vignettes” and image characteristics of all objects were
201 extracted with ZooProcess (Gorsky et al., 2010) and sorted into 39 categories using Plankton
202 Identifier (Gasparini, 2007). Automated image sorting was then manually validated by
203 experts.

204

205 **3 Results**

206 **3.1 Hydrography**

207 The site survey with RV Meteor succeeded in sampling the eddy core with CTD and UVP
208 casts. The lowest measured O₂ concentration was 3.75 µmol O₂ kg⁻¹ at 106 m depth. Based
209 upon the current velocity, the eddy was approximately 110 km in diameter (Fig. 1), but
210 oxygen concentrations below 20 and 5 µmol O₂ kg⁻¹ were only found within approximately
211 18 and 8 km from the center, respectively. For the purpose of this study, the four stations
212 within 20 km to the eddy core (with minimum O₂ concentrations well below 20 µmol O₂ kg⁻¹)
213 were considered “eddy core”, while the four stations within 20 to 35 km from the eddy core
214 were considered “eddy margin” (with minimum O₂ concentrations between 21 and 53 µmol
215 O₂ kg⁻¹) and the CVOO station (M105 data complemented with data from previous cruises,

216 n=7 profiles, see methods) was considered to represent ambient conditions outside of the
217 eddy. Here, a shallow OMZ was not present. The midwater OMZ (centered around
218 approximately 450 m depth) featured mean minimum oxygen concentrations of $70 \mu\text{mol O}_2$
219 kg^{-1} .

220

221 **3.2 Vertical distribution and DVM – acoustic observations**

222 During the M105 ADCP survey, several features were apparent in the vertical distribution and
223 migration of scatterers outside of the eddy (Fig. 2). First, a deep scattering layer was detected
224 centered between below 350 and 400 m depth. From this layer, part of the population started
225 its ascent to the surface layer at about 18:00 UTC. The center of the nighttime distribution
226 outside the eddy ranged from approximately 30 to 130 m depth. During the day, lowest S_v
227 was recorded between 100 and 300 m depth, with a residual non-migrating population in the
228 upper 100 m. The ascendant and descendent migration took place from approximately 18:00
229 to 20:00 UTC (16:15 to 18:15 solar time) and 07:00 to 09:00 UTC (05:15 to 07:17 solar
230 time), respectively.

231 A very different nighttime distribution was observed when traversing the eddy. The scatterers
232 in the surface layer were located further up in the water column than outside the eddy and
233 their lower distribution margin coincided with the upper oxycline (approximately 85 m in the
234 eddy center). In the core of the shallow OMZ, below approximately $20 \mu\text{mol O}_2 \text{ kg}^{-1}$, an
235 absolute minimum S_v was observed.

236 The intersection of the two transects (see red crosses in Fig. 2) was visited shortly after 12:00
237 and 00:00 UTC, representing full day/night conditions, respectively. Here, the difference
238 between S_v in the surface at day and night suggests substantial vertical migration into/out of
239 the surface layer, crossing the OMZ (Fig 2.b). Also, the distribution of the surface daytime
240 resident population (with S_v values of approximately 75dB) is bimodal, peaking again at
241 approximately 90 m. This is well within the shallow OMZ (note that there are no O_2 isolines
242 shown in the daytime transect in Fig. 2b since there were no CTD casts performed on the first
243 transect).

244 Reanalysis of acoustic backscatter and oxygen time series data from the CVOO mooring
245 before and during the transit of an ACME in 2010 (Karstensen et al. 2015) shows that the

246 daytime S_v at the depth level of the oxygen sensor (around 50 m, depending on wire angle) is
247 reduced below approximately $20 \mu\text{mol O}_2 \text{ kg}^{-1}$ (Fig. 3a, power function; $r^2=0.69$). For the
248 nighttime data (Fig. 3b), the relationship between S_v and oxygen concentration is best
249 described by a linear function ($r^2=0.94$). S_v in the subsurface increases around approximately
250 07:00 and 19:00 UTC (supplementary figure S1). These dusk and dawn traces suggest that
251 DVM species migrate through the OMZ even when the daily mean oxygen concentration is
252 between 5 and $20 \mu\text{mol kg}^{-1}$.

253 3.3 Optical Profiling

254 The UVP5 transect across the eddy revealed a pronounced increase of aggregates in the eddy
255 core (Fig. 4a). This pattern was still evident at the maximum profile depth (600 m, below the
256 midwater OMZ). At the same time, surface abundance of copepods (Fig. 4b) and, to a lesser
257 degree, collodaria (Fig. 4c) is higher than in surrounding waters. Copepods were observed in
258 substantial abundance within the OMZ, while collodaria appeared to avoid it. On the other
259 hand, gelatinous zooplankton (comprising medusae, ctenophores, and siphonophores, Fig. 3d)
260 were observed in the inner OMZ core. Not a single observation of shrimp-like micronekton
261 (euphausiids and decapods, Fig. 4e) was made at oxygen concentrations lower than $28 \mu\text{mol}$
262 $\text{O}_2 \text{ kg}^{-1}$. Integrated abundance (upper 600 m, Fig. 5) of large aggregates was significantly
263 higher in the “core” stations compared to the “outside” (one-way ANOVA, Tukey’s HSD
264 $p<0.001$) and “margin” ($p<0.05$) stations. The integrated abundance of gelatinous plankton
265 was significantly higher in the “core” stations than in the “outside” stations ($p<0.05$). For the
266 other groups, differences in integrated abundance were not significant.

267 3.4 Multinet

268 The multinet data provides a higher taxonomic resolution, but lower spatial (horizontal and
269 vertical) resolution than the optical profiles (UVP). In Fig. 6, the abundance and vertical
270 distribution of eight conspicuous taxa are depicted, ordered by their apparent sensitivity to
271 hypoxia. While euphausiids (Fig. 6a), calanoid copepods (Fig. 6b) and foraminifera (Fig. 6c)
272 are abundant in the surface layer (exceeding the mean abundance at CVOO), they appear to
273 avoid the shallow OMZ. Siphonophores (Fig. 6d), the poecilostomatoid *Oncaea* spp. (Fig. 6e)
274 and eucalanoid copepods (Fig. 6f) are all very abundant in the eddy’s surface layer during the
275 night (with the latter also being observed in the shallow OMZ during nighttime) and appear to

276 take refuge within the shallow OMZ during daylight hours. Two groups that appeared to
277 favour the shallow OMZ even during nighttime hours were polychaetes (Fig. 6g) and
278 ostracods (Fig. 6h), but also the harpacticoid copepod *Macrosetella gracilis* (Table S1). Taxa
279 that were more abundant in the surface layer of the eddy core compared to the mean outside
280 eddy situation, included eucalanoid and other calanid copepods, *Oithona* spp., *Macrosetella*
281 *gracilis*, *Oncaea* spp., ostracods, decapods, siphonophores, chaetognaths, molluscs (mainly
282 pteropods), polychaetes and foraminifera (Table S1). In contrast, taxa that were less abundant
283 in the surface layer in the eddy were amphipods, salps and appendicularia. Although not
284 sampled quantitatively by this type of net, this also seemed to be the case for fishes. In
285 particular, no single individual was caught in the upper 200 m of the eddy core night station.
286 Total area-integrated abundance of all zooplankton organisms in the upper 600 m was
287 151,000(\pm 34,000) m⁻² in the eddy core and 101,000(\pm 15,000) at the “outside” station (Table
288 S2).

289

290 **4 Discussion**

291 Already during the remote survey, it became apparent that the tracked mesoscale eddy was a
292 hotspot of primary productivity. Lowered sea surface temperature and elevated surface chl-*a*
293 values (satellite imagery; Schütte et al., 2015a) as well as increased nitrate levels in the eddy
294 interior (autonomous gliders; Karstensen et al., 2016, Fiedler et al., 2016) indicate active
295 upwelling and translate into substantially increased productivity (Löscher et al., 2015).
296 During westward propagation, the hydrographic character was found to be remarkably
297 constant (Karstensen et al., 2016; Schütte et al., 2016), while the genomic characterization
298 (Löscher et al., 2015) as well as the particle composition (Fischer et al., 2015) indicate that
299 the eddy has created a unique ecosystem that has not much in common with the coastal one it
300 originated from. The present study is the first to observe the impact of such eddies on pelagic
301 metazoans. Since process understanding and zooplankton production estimates are still
302 lacking, we cannot conclude whether the system is ultimately bottom-up or top-down
303 controlled and whether the seemingly high zooplankton productivity may be due to lacking
304 higher trophic levels.

305 We deliberately chose not to attempt a direct comparison of methods (e.g. by trying to derive
306 biomass from ADCP backscatter), but rather use the three methods complementary to each

307 other: The acoustic survey reveals the horizontal and vertical fine-scale spatial distribution of
308 scatterers (macrozooplankton and micronekton). It suggests a complete avoidance of the
309 OMZ by these groups, whose identity remains somewhat unclear (see also Karstensen et al.,
310 2015). The UVP has an excellent vertical and an intermediate horizontal (several profiles
311 along transect) resolution, with restricted information regarding the identity of the organisms
312 (limited by image resolution and sampling volume to more abundant mesozooplankton). The
313 multinet has low vertical and horizontal resolution, and low catch efficiency for fast-
314 swimming organisms. Its main asset is that it allows a detailed investigation of zooplankton
315 and some micronekton organisms. Since the samples are still intact after scanning,
316 taxonomists interested in one of the groups presented here would even be able proceed with
317 more detailed work.

318 Using the shipboard and moored ADCP to investigate acoustic backscatter (rather than a
319 calibrated scientific echosounder) resulted from the necessity to gather ADCP-derived current
320 velocity data for eddy identification and localization of the core (see Fig. 1). It has to be noted
321 that the backscatter signals from the 75kHz shipboard ADCP and the 300 KHz moored ADCP
322 are strictly not comparable as for organisms that are small compared to the acoustic
323 wavelengths, the backscatter strength increases rapidly with increasing frequency (Stanton et
324 al., 1994). Also, smaller organisms contribute more to the 300 kHz signal than to the 75 kHz.
325 Still, both instruments suggest that OMZ avoidance sets in at O₂ concentrations lower than
326 approximately 20 μmol O₂ kg⁻¹.

327 The marked decrease in ADCP S_v in the shallow OMZ is only partly confirmed by the other
328 two techniques. The animals that contribute most to the ADCP backscatter at a frequency of
329 75 kHz are targets in the cm-size range (75kHz correspond to a wavelength of 20 mm), i.e.
330 larger zooplankton and micronekton such as euphausiids, amphipods, small fish, pteropods,
331 siphonophores and large copepods (Ressler, 2002). Thus, the community of organisms
332 contributing most to the backscatter is not quantitatively (i.e., providing accurate abundance
333 estimates) sampled by the multinet and the UVP5. Both mostly target organisms < 10 mm in
334 size and the sampling volume is small, in particular with the UVP5. Still, spatial observation
335 patterns of these organisms derived from the multinet and UVP5 may help to provide
336 explanations for the patterns observed in the ADCP, even though abundance estimates are to
337 be taken with caution. For example, euphausiids contribute substantially to the backscatter at
338 75kHz in this region (as observed through horizontal MOCNESS tows during dusk and dawn

339 resolving ADCP migration traces, Buchholz, Kiko, Hauss, Fischer unpubl.). Thus, the relative
340 decrease of observed euphausiids in the OMZ (and in the eddy in general) in both multinet
341 samples and UVP profiles suggests that they may be partly responsible for the lack of
342 backscatter in the OMZ.

343 High-resolution profiles obtained by the UVP5 indicated OMZ avoidance by euphausiids and
344 collodaria, while copepods (albeit at lower concentrations than in the surface layer) were
345 observed in the OMZ core. Gelatinous zooplankton was even more abundant in the shallow
346 OMZ than in surface waters. The multinet data (providing higher taxonomic resolution and
347 larger sampling volume, but lower vertical resolution) suggest that there are four strategies
348 followed by zooplankton in the eddy, which will be discussed below.

349 *i) shallow OMZ avoidance and compression at the surface*

350 We ascribe this behaviour to euphausiids and most calanoid copepods as well as collodaria
351 and foraminifera (from the supergroup rhizaria). While the total abundance of krill is probably
352 underestimated by the comparatively slow and small plankton net, their vertical distribution in
353 relation to the OMZ and the marked total decrease within the eddy compared to “outside”
354 stations suggests that they are susceptible to OMZ conditions and may suffer from increased
355 predation in the surface layer. This is in line with physiological observations, where a critical
356 partial pressure of 2.4 and 6.2 kPa (29.6 and 64.2 $\mu\text{mol O}_2 \text{ kg}^{-1}$) was determined at subsurface
357 (13°C) and near-surface temperature (23°C), respectively, in *Euphausia gibboides* in the
358 ETNA (Kiko et al., 2015). Calanoid copepods represent the largest group in terms of
359 abundance and biomass and comprise approximately one hundred species in Cape Verdean
360 waters (Séguin, 2010) with a wide range of physiological and behavioural adaptations.
361 Species most tolerant to low-oxygen conditions are vertically migrating species such as
362 *Pleuromamma* spp., while epipelagic species such as *Undinula vulgaris* are less tolerant
363 (Teuber et al., 2013; Kiko et al., 2015). From the rhizaria supergroup, the fine-scale
364 distribution pattern of solitary collodaria (a group that is abundant in surface waters of the
365 oligotrophic open ocean, see Biard et al., 2015 and references therein) suggests OMZ
366 sensitivity, but direct evidence from the literature is lacking. The foraminifera, which are
367 mostly too small to be quantified well with the UVP5, but in contrast to other rhizaria are well
368 preserved in buffered formaldehyde in seawater solution, were highly abundant in the surface
369 of the eddy core. Here, the distribution shift likely also includes a community shift, since a
370 marked dominance change from surface-dwelling to subsurface-dwelling species was found

371 in sediment trap data during the transit of the 2010 ACME (Fischer et al., 2015). In that
372 ACME, also an export flux peak by foraminifera was observed.

373 *ii) migration to the shallow OMZ core during daytime*

374 This strategy seems to be followed by siphonophores, *Oncaea* spp., and eucalanoid copepods.
375 Although it seems unlikely that siphonophores in this survey were contributing substantially
376 to the ADCP backscatter, as those retrieved by the multinet were almost exclusively
377 calycothorans (see Fig. 6d for a type specimen) which do not have a pneumatophore and,
378 therefore, lack gas bubbles that are highly resonant in other siphonophore groups (e.g.
379 Ressler, 2002). They may, however, contribute to the weak backscatter signal in the shallow
380 OMZ during daytime (Fig. 2b and 6d). *Oncaea* spp. are particle-feeding copepods that are
381 directly associated with marine snow (Dagg et al., 1980). They were observed in quite
382 extreme OMZs in other oceanic regions (e.g. Böttger-Schnack, 1996; Saltzman & Wishner,
383 1997), however, our results suggest that at least in the tropical Atlantic biome they cannot
384 permanently endure hypoxia but have to pay their oxygen debt during nighttime. The majority
385 of adult eucalanoid copepods were *Rhincalanus nasutus*, a species that is frequently found in
386 the midwater OMZ of the ETNA. In the eastern tropical Pacific, however, *R. nasutus* was
387 reported to be excluded from the extreme midwater OMZ (500-1000 m depth, below
388 approximately 22 $\mu\text{mol O}_2 \text{ kg}^{-1}$), unlike the key OMZ-adapted eucalanoid species of that
389 region (e.g. *Eucalanus inermis*), which are able to permanently inhabit the OMZ (Saltzman &
390 Wishner, 1997). In our study, *R. nasutus* were found also in the shallow (extreme) OMZ of
391 the eddy (well below 20 $\mu\text{mol O}_2 \text{ kg}^{-1}$), indicating that this copepod species may be also able
392 to cope with further deoxygenation of the midwater OMZ in the Atlantic. Both *Oncaea* and
393 *Rhincalanus* are unlikely to be seen in the S_v signal at 75 kHz.

394 *iii) residing in the shallow OMZ day and night*

395 Contrary to most crustaceans, collodaria and euphausiids, a remarkable ability to endure OMZ
396 conditions for prolonged periods of time seems to be present in ostracods, polychaetes,
397 *Macrosetella gracilis* and gelatinous plankton. “Jellies” are a group of organisms of which
398 several taxa, such as siphonophores, salps, hydromedusae and ctenophores, have been
399 reported to tolerate hypoxic conditions much better than most crustacean zooplankton (Mills
400 2001; Thuesen et al. 2005). In addition to reduced metabolic activity (e.g. Rutherford and
401 Thuesen, 2005), using the mesoglea gel matrix as an oxygen reservoir was shown to be a
402 strategy in scyphomedusae to temporarily survive anoxia (Thuesen et al. 2005). It has also

403 been suggested that “jellyfish” (i.e., pelagic cnidarians and ctenophores) outcompete other
404 planktonic groups in coastal systems under eutrophication-induced hypoxia (Mills 2001). The
405 UVP5 nighttime section suggests that many gelatinous organisms reside within the shallow
406 OMZ even during nighttime. This is only partly confirmed by the multinet data; however,
407 ctenophores and medusae are often destroyed during sampling and not well preserved in
408 formaldehyde. For ostracods, it is known that several limnic (Teixeira et al. 2014) and marine
409 (Corbari et al. 2004) benthic species tolerate hypoxia for prolonged periods of time (and
410 preferentially select hypoxic habitats over oxygenated ones), which lead to the use of their
411 abundance in sediment cores as a proxy for past ocean oxygenation (Lethiers and Whatley,
412 1994). In pelagic marine ostracods, however, there is little evidence for particular
413 preadaptation to OMZ conditions. To the best of our knowledge, no physiological studies
414 exist that describe the metabolic response of pelagic ostracods to hypoxia. Recently, it was
415 found that the oxygen transport protein hemocyanin occurs in several groups within the class
416 ostracoda, including planktonic species (Marxen et al. 2014). In the Arabian Sea, highest
417 ostracod abundances were found in the oxygenated surface layer, but consistent occurrence in
418 the extreme OMZ ($<5 \mu\text{mol O}_2 \text{ kg}^{-1}$) was reported (Böttger-Schnack, 1996). In the eastern
419 tropical Pacific, most species were reported to avoid the OMZ, with the notable exception of
420 *Conchoecetta giesbrechti*, which is classified as an OMZ-adapted species (Castillo et al.,
421 2007). For pelagic polychaetes, Thuesen and Childress (1993) even state that they may have
422 the highest metabolic rates (and, thus, oxygen demand) in the meso- and bathypelagic zones
423 of the oceans, with the exception of the aberrant species *Poeobius meseres*.

424 *iv) migration through the shallow OMZ core to better-oxygenated depths*

425 To rigorously assess DVM reduction by the underlying OMZ, acoustic 24h-observations
426 would be necessary to directly observe the migration pattern. Unfortunately, the dawn and
427 dusk migration observations took place at the NE- and SW-margin of the eddy, respectively,
428 just outside the $30 \mu\text{mol O}_2 \text{ kg}^{-1}$ boundary (Fig. 2). Nevertheless, it appears from the
429 day/night difference in the shipboard ADCP S_v (at the intersection of the two transects) as
430 well as from the moored ADCP data (Fig S1) that at least part of the migrating population
431 “holds its breath” and crosses the OMZ during ascent/descent. In this respect, the thin shallow
432 OMZ seems to be different from the several hundred meters thick mesopelagic OMZ, which
433 at low core oxygen concentrations can serve as a quite effective migration barrier (Auel and
434 Verheye, 2007; Teuber et al., 2013).

435 The enhanced surface primary productivity of the eddy also resulted in an approximately 5-
436 fold increase of large particles, well visible down to 600 m depth. This indicates a massive
437 export flux by sinking marine snow (see also Fischer et al. 2015 for sediment trap data of the
438 2010 ACME), which is thus made available to higher trophic levels at greater depths. As an
439 example, phaeodaria (in supergroup rhizaria) are one of the few exclusively mesopelagic
440 groups (only found deeper than approximately 200 m in UVP profiles). Their integrated
441 abundance of seemed to be positively affected by the eddy conditions, which may indicate
442 favourable feeding/growth conditions at depth.

443 In summary, mesozooplankton biomass was generally enhanced in the euphotic zone of the
444 ACME, suggesting that it may represent an “oasis in the desert” *sensu* Godø et al. (2012),
445 although the differences to “outside” conditions were not quite as large as those reported by
446 Goldthwait and Steinberg (2008). On the other hand, subsurface hypoxia appears to be
447 detrimental to some surface-dwelling as well as vertically migrating zooplankton taxa. We
448 lack quantitative estimates of higher trophic levels (the multinet is too small and slow to
449 efficiently sample fast-swimming nekton organisms), but it seems that the small migratory
450 mesopelagic fishes which were usually caught (albeit in low numbers) outside the eddy were
451 less abundant in the eddy core’s surface. To draw robust conclusions on the identity and
452 whereabouts of acoustic scatterers, the additional use of several types of stratified nets is
453 necessary (e.g. 10 m² MOCNESS in addition to a multinet or 1 m² MOCNESS) but was
454 logistically impossible during the opportunistic sampling on M105. Since gelatinous plankton
455 organisms appear to play a key role in these oceanic OMZs and are notoriously undersampled
456 by nets and/or destroyed by fixatives, it even seems worthwhile to employ a dedicated camera
457 system (with larger sampling volume than the UVP5) for such a survey. It also remains an
458 open question whether the rich zooplankton prey field is exploited by epipelagic fishes and
459 their predators (see e.g. Tew Kai and Marsac, 2010 for examples of tuna and seabird
460 interaction with cyclonic eddies). By providing isolated bodies of water with distinct (and
461 sometimes, like in our case, extreme) environmental conditions for many months, mesoscale
462 eddies are important vectors of species dispersal and invasion (Wiebe and Flierl, 1983) and
463 subject the population fragments they contain to their own mutations, selection forces, and
464 genetic drift effects. Thus, they are not only hypothesized to play a central role in speciation
465 of planktonic species (Bracco et al. 2000, Clayton et al. 2013), but may resemble a key

466 mechanism to equip oceanic metapopulations with the range of physiological and behavioural
467 adaptations deemed necessary to survive under global change.

468

469 **5 Conclusions**

470 Acoustic observations (shipboard ADCP) confirm previous observations (moored ADCP) of a
471 sharp decrease in backscatter at O₂ concentrations below approximately 20 μmol O₂ kg⁻¹.
472 Euphausiids (which are known to contribute substantially to the ADCP backscatter) were not
473 observed within the OMZ stratum of the eddy, and their integrated abundance was markedly
474 reduced. Still, multinet and UVP5 data indicate that several zooplankton groups are
475 surprisingly insensitive to these extreme OMZ conditions, and many taxa that avoid the OMZ
476 even reach higher abundance in the productive surface environment of the eddy. However, it
477 remains an open question if and how higher trophic levels (such as small pelagic forage fish
478 and their predators) may benefit from the dense prey field. While the term “open ocean dead
479 zone” may be an exaggeration, low-oxygen eddies in the ETNA in the light of future
480 deoxygenation might serve as a crystal ball (or, more appropriately, a “screaming pool”) to
481 estimate the differential response of different plankton functional groups of the open ocean to
482 global change.

483

484 **Acknowledgements**

485 We are particularly grateful to the chief scientists of M105, Martin Visbeck and Toste
486 Tanhua, for shaving two days off their tight cruise schedule to make this survey happen. This
487 work is a contribution of the Future Ocean Excellence Cluster project CP1341
488 “Biogeochemistry and Ecology of Oxygen Depleted Eddies in the Eastern Tropical Atlantic”
489 and of the SFB 754 "Climate - Biogeochemistry Interactions in the Tropical Ocean"
490 (www.sfb754.de) which is supported by the German Science Foundation (DFG).

491

492 **References**

493 Andersen, V., Sardou, J., and Gasser, B.: Macroplankton and micronekton in the northeast
494 tropical Atlantic: abundance, community composition and vertical distribution in relation to

495 different trophic environments, *Deep Sea Research Part I: Oceanographic Research Papers*,
496 44, 193-222, 1997.

497 Auel, H. and Verheye, H. M.: Hypoxia tolerance in the copepod *Calanoides carinatus* and the
498 effect of an intermediate oxygen minimum layer on copepod vertical distribution in the
499 northern Benguela Current upwelling system and the Angola–Benguela Front, *Journal of*
500 *Experimental Marine Biology and Ecology*, 352, 234-243, 2007.

501 Biard, T., Pillet, L., Decelle, J., Poirier, C., Suzuki, N., and Not, F.: Towards an Integrative
502 Morpho-molecular Classification of the Collodaria (Polycystinea, Radiolaria), *Protist*,
503 doi:10.1016/j.protis.2015.05.002, 2015.

504 Böttger-Schnack, R.: Vertical structure of small metazoan plankton, especially noncalanoid
505 copepods. I. Deep Arabian Sea, *Journal of Plankton Research*, 18, 1073-1101, 1996.

506 Bracco, A., Provenzale, A., and Scheuring, I.: Mesoscale vortices and the paradox of the
507 plankton, *Proceedings of the Royal Society of London B: Biological Sciences*, 267, 1795-
508 1800, 2000.

509 Castillo, R., Antezana, T., and Ayon, P.: The influence of El Niño 1997–98 on pelagic
510 ostracods in the Humboldt Current Ecosystem off Peru, *Hydrobiologia*, 585, 29-41, 2007.

511 Clayton, S., Dutkiewicz, S., Jahn, O., and Follows, M. J.: Dispersal, eddies, and the diversity
512 of marine phytoplankton, *Limnology and Oceanography: Fluids and Environments*, 3, 182-
513 197, 2013.

514 Cocco, V., Joos, F., Steinacker, M., Frölicher, T., Bopp, L., Dunne, J., Gehlen, M., Heinze,
515 C., Orr, J., and Oeschlies, A.: Oxygen and indicators of stress for marine life in multi-model
516 global warming projections, *Biogeosciences*, 10, 1849-1868, 2013.

517 Corbari, L., Carbonel, P., and Massabuau, J.-C.: How a low tissue O₂ strategy could be
518 conserved in early crustaceans: the example of the podocopid ostracods, *Journal of*
519 *experimental biology*, 207, 4415-4425, 2004.

520 Dagg, M., Cowles, T., Whitley, T., Smith, S., Howe, S., and Judkins, D.: Grazing and
521 excretion by zooplankton in the Peru upwelling system during April 1977, *Deep Sea Research*
522 *Part I: Oceanographic Research Papers*, 27, 43-59, 1980.

523 Deimes, K.L., Backscatter Estimation Using Broadband Acoustic Doppler Current Profilers,
524 Proceedings of the IEEE Sixth Working Conference on Current Measurement, San Diego,
525 CA, March 11-13 1999. pp.249-253, DOI: 10.1109/CCM.1999.755249, 1999.

526 Fiedler, B., Grundle, D., Schütte, F., Karstensen, J., Löscher, C. R., Hauss, H., Wagner, H.,
527 Loginova, A., Kiko, R., Silva, P., and Körtzinger, A.: Oxygen Utilization and Downward
528 Carbon Flux in an Oxygen-Depleted Eddy in the Eastern Tropical North Atlantic,
529 Biogeosciences Discuss., 2016, 1-35, 2016.

530 Fischer, J., Brandt, P., Dengler, M., Müller, M., and Symonds, D.: Surveying the upper ocean
531 with the Ocean Surveyor: a new phased array Doppler current profiler, Journal of
532 Atmospheric and Oceanic Technology, 20, 742-751, 2003.

533 Fischer, G., Karstensen, J., Romero, O., Baumann, K-H., Donner, B., Hefter, J., Mollenhauer,
534 G., Iversen, M., Fiedler, B., Monteiro, I. and Körtzinger, A.: Bathypelagic particle flux
535 signatures from a suboxic eddy in the oligotrophic tropical North Atlantic: production,
536 sedimentation and preservation, Biogeosciences Discuss., 12, 18253-18313, 2015..

537 Gasparini, S.: PLANKTON IDENTIFIER: a software for automatic recognition of planktonic
538 organisms. http://www.obs-vlfr.fr/~gaspari/Plankton_Identifier/index.php, last access
539 11/11/2015, 2007.

540 Godø, O. R., Samuelsen, A., Macaulay, G. J., Patel, R., Hjøllø, S. S., Horne, J., Kaartvedt, S.,
541 and Johannessen, J. A.: Mesoscale eddies are oases for higher trophic marine life, PLoS One,
542 7, e30161, doi: 10.1371/journal.pone.0030161, 2012.

543 Goldthwait, S. A. and Steinberg, D. K.: Elevated biomass of mesozooplankton and enhanced
544 fecal pellet flux in cyclonic and mode-water eddies in the Sargasso Sea, Deep Sea Research
545 Part II: Topical Studies in Oceanography, 55, 1360-1377, 2008.

546 Gorsky, G., Ohman, M. D., Picheral, M., Gasparini, S., Stemann, L., Romagnan, J.-B.,
547 Cawood, A., Pesant, S., García-Comas, C., and Prejger, F.: Digital zooplankton image
548 analysis using the ZooScan integrated system, Journal of Plankton Research, 32, 285-303,
549 2010.

550 Karstensen, J., Stramma, L., and Visbeck, M.: Oxygen minimum zones in the eastern tropical
551 Atlantic and Pacific oceans, Progress in Oceanography, 77, 331-350, 2008.

552 Karstensen, J., Fiedler, B., Schütte, F., Brandt, P., Körtzinger, A., Fischer, G., Zantopp, R.,
553 Hahn, J., Visbeck, M., and Wallace, D.: Open ocean dead zones in the tropical North Atlantic
554 Ocean, *Biogeosciences*, 12, 2597-2605, 2016.

555 Karstensen, J., Schütte, F., Pietri, A., Krahnemann, G., Fiedler, B., Grundle, D., Hauss, H.,
556 Körtzinger, A., Löscher, C., and Viera, N.: Anatomy of open ocean dead-zones based on
557 high-resolution multidisciplinary glider data, *Biogeosciences Discuss.*, 2016.

558 Kiko, R., Hauss, H., Buchholz, F., and Melzner, F.: Ammonium excretion and oxygen
559 respiration of tropical copepods and euphausiids exposed to oxygen minimum zone
560 conditions, *Biogeosciences Discuss.*, 12, 17329-17366, 2015.

561 Kinzer, J. and Schulz, K.: Vertical distribution and feeding patterns of midwater fish in the
562 central equatorial Atlantic, *Marine Biology*, 85, 313-322, 1985.

563 Lethiers, F. and Whatley, R.: The use of Ostracoda to reconstruct the oxygen levels of Late
564 Palaeozoic oceans, *Marine Micropaleontology*, 24, 57-69, 1994.

565 Löscher, C. R., Fischer, M. A., Neulinger, S. C., Fiedler, B., Philippi, M., Schütte, F., Singh,
566 A., Hauss, H., Karstensen, J., Körtzinger, A., Künzel, S., and Schmitz, R. A.: Hidden
567 biosphere in an oxygen-deficient Atlantic open-ocean eddy: future implications of ocean
568 deoxygenation on primary production in the eastern tropical North Atlantic, *Biogeosciences*,
569 12, 7467-7482, 2015.

570 MacLennan, D. N., Fernandes, P. G., and Dalen, J.: A consistent approach to definitions and
571 symbols in fisheries acoustics, *ICES Journal of Marine Science*, 59, 365-369, 2002.

572 Marxen, J., Pick, C., Oakley, T., and Burmester, T.: Occurrence of Hemocyanin in Ostracod
573 Crustaceans, *J Mol Evol*, 79, 3-11, 2014.

574 McGillicuddy, D. J., Anderson, L. A., Bates, N. R., Bibby, T., Buesseler, K. O., Carlson, C.
575 A., Davis, C. S., Ewart, C., Falkowski, P. G., and Goldthwait, S. A.: Eddy/wind interactions
576 stimulate extraordinary mid-ocean plankton blooms, *Science*, 316, 1021-1026, 2007.

577 Menkes, C. E., Kennan, S. C., Flament, P., Dandonneau, Y., Masson, S., Biessy, B., Marchal,
578 E., Eldin, G., Grelet, J., and Montel, Y.: A whirling ecosystem in the equatorial Atlantic,
579 *Geophysical Research Letters*, 29, 48-41-48-44, 2002.

580 Mills, C.: Jellyfish blooms: are populations increasing globally in response to changing ocean
581 condition?, *Hydrobiologia*, 451, 55-68, 2001.

582 Palacios, D. M., Bograd, S. J., Foley, D. G., and Schwing, F. B.: Oceanographic
583 characteristics of biological hot spots in the North Pacific: A remote sensing perspective,
584 Deep Sea Research Part II: Topical Studies in Oceanography, 53, 250-269, 2006.

585 Picheral, M.G., Stemmann, L., Karl, D.M., Iddaoud, G., Gorsky, G. The Underwater Vision
586 Profiler 5: An advanced instrument for high spatial resolution studies of particle size spectra
587 and zooplankton. Limnol Oceanogr Methods 8: 462-473. doi: 10.4319/lom.2010.8.462, 2010

588 Postel, L., da Silva, A. J., Mohrholz, V., and Lass, H.-U.: Zooplankton biomass variability off
589 Angola and Namibia investigated by a lowered ADCP and net sampling, Journal of Marine
590 Systems, 68, 143-166, 2007.

591 Prince, E. D., Luo, J. C., Goodyear, P., Hoolihan, J. P., Snodgrass, D., Orbesen, E. S., Serafy,
592 J. E., Ortiz, M., and Schirripa, M. J.: Ocean scale hypoxia based habitat compression of
593 Atlantic istiophorid billfishes, Fisheries Oceanography, 19, 448-462, 2010.

594 Ressler, P. H.: Acoustic backscatter measurements with a 153kHz ADCP in the northeastern
595 Gulf of Mexico: determination of dominant zooplankton and micronekton scatterers, Deep
596 Sea Research Part I: Oceanographic Research Papers, 49, 2035-2051, 2002.

597 Rutherford Jr, L. D. Thuesen, E.V.: Metabolic performance and survival of medusae in
598 estuarine hypoxia, Marine Ecology Progress Series, 294, 189-200, 2005.

599 Saltzman, J. and Wishner, K. F.: Zooplankton ecology in the eastern tropical Pacific oxygen
600 minimum zone above a seamount: 2. Vertical distribution of copepods, Deep Sea Research
601 Part I: Oceanographic Research Papers, 44, 931-954, 1997.

602 Schütte, F., Brandt, P., and Karstensen, J.: Occurrence and characteristics of mesoscale eddies
603 in the tropical northeast Atlantic Ocean, Ocean Science Discussions, 12, 3043-3097, 2015.

604 Schütte, F., Karstensen, J., Krahnemann, G., Fiedler, B., Brandt, P., Visbeck, M., and
605 Körtzinger, A.: Characterization of “dead-zone eddies” in the tropical North Atlantic Ocean,
606 Biogeosciences Discuss., 2016.

607 Séguin, F.: Zooplankton community near the island of São Vicente in the Cape Verde
608 archipelago: insight on pelagic copepod respiration, MSc Thesis, University of Bremen, 77
609 pp., 2010.

610 Stanton, T. K., Wiebe, P. H., Chu, D., Benfield, M. C., Scanlon, L., Martin, L., and Eastwood,
611 R. L.: On acoustic estimates of zooplankton biomass, *ICES Journal of Marine Science*, 51,
612 505-512, 1994.

613 Stramma, L., Johnson, G. C., Sprintall, J., and Mohrholz, V.: Expanding Oxygen-Minimum
614 Zones in the Tropical Oceans, *Science*, 320, 655-658, 2008.

615 Stramma, L., M. Visbeck, P. Brandt, T. Tanhua, and D. Wallace: Deoxygenation in the
616 oxygen minimum zone of the eastern tropical North Atlantic, *Geophys. Res. Lett.*, 36,
617 L20607, doi:10.1029/2009GL039593, 2009.

618 Stramma, L., Prince, E. D., Schmidtko, S., Luo, J., Hoolihan, J. P., Visbeck, M., Wallace, D.
619 W., Brandt, P., and Körtzinger, A.: Expansion of oxygen minimum zones may reduce
620 available habitat for tropical pelagic fishes, *Nature Climate Change*, 2, 33-37, 2012.

621 Stramma, L., Bange, H. W., Czeschel, R., Lorenzo, A., and Frank, M.: On the role of
622 mesoscale eddies for the biological productivity and biogeochemistry in the eastern tropical
623 Pacific Ocean off Peru, *Biogeosciences*, 10, 7293-7306, 2013.

624 Teixeira, M. C., Budd, M. P., and Strayer, D. L.: Responses of epiphytic aquatic
625 macroinvertebrates to hypoxia, *Inland Waters*, 5, 75-80, 2014.

626 Teuber, L., Schukat, A., Hagen, W., and Auel, H.: Distribution and ecophysiology of calanoid
627 copepods in relation to the oxygen minimum zone in the eastern tropical Atlantic, *PloS one*,
628 8, e77590, doi: 10.1371/journal.pone.0077590, 2013.

629 Tew Kai, E. and Marsac, F.: Influence of mesoscale eddies on spatial structuring of top
630 predators' communities in the Mozambique Channel, *Progress in Oceanography*, 86, 214-223,
631 2010.

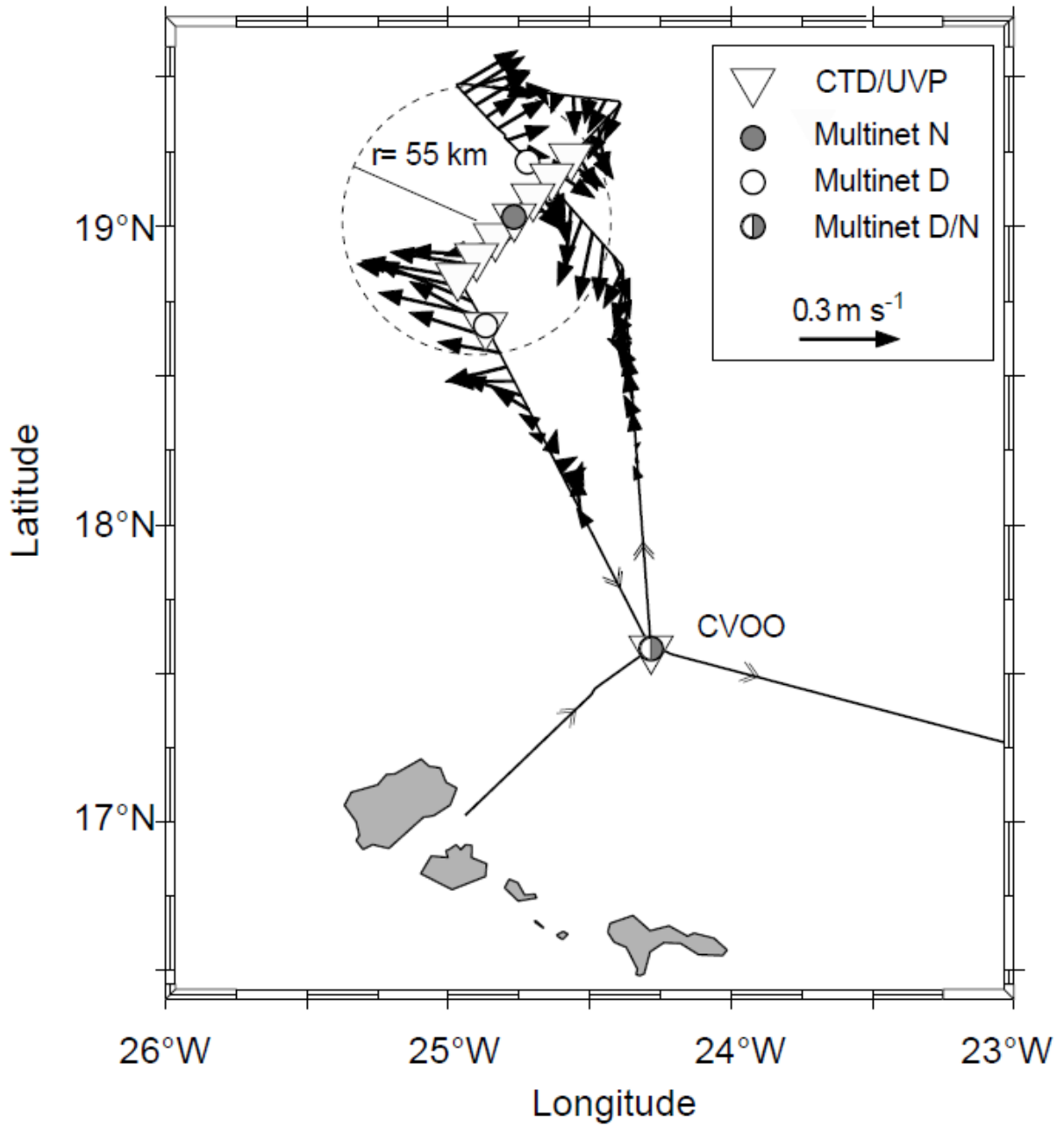
632 Thuesen, E. V. and Childress, J. J.: Metabolic rates, enzyme activities and chemical
633 compositions of some deep-sea pelagic worms, particularly *Nectonemertes mirabilis*
634 (*Nemertea*; *Hoploneuridae*) and *Poebius meseres* (*Annelida*; *Polychaeta*), *Deep Sea*
635 *Research Part I: Oceanographic Research Papers*, 40, 937-951, 1993.

636 Thuesen, E. V., Rutherford, L. D., Brommer, P. L., Garrison, K., Gutowska, M. A., and
637 Towanda, T.: Intragel oxygen promotes hypoxia tolerance of scyphomedusae, *Journal of*
638 *Experimental Biology*, 208, 2475-2482, 2005.

- 639 Tremblay, N., Zenteno-Savín, T., Gómez-Gutiérrez, J., and Maeda-Martínez, A. N.:
640 Migrating to the Oxygen Minimum Layer: Euphausiids. In: *Oxidative Stress in Aquatic*
641 *Ecosystems*, John Wiley and Sons, Ltd, pp. 89-98, doi: 10.1002/9781444345988.ch6, 2011.
- 642 Wiebe, P. and Flierl, G.: Euphausiid invasion/dispersal in Gulf Stream cold-core rings,
643 *Australian Journal of Marine and Freshwater Research*, 34, 625-652, 1983.

644

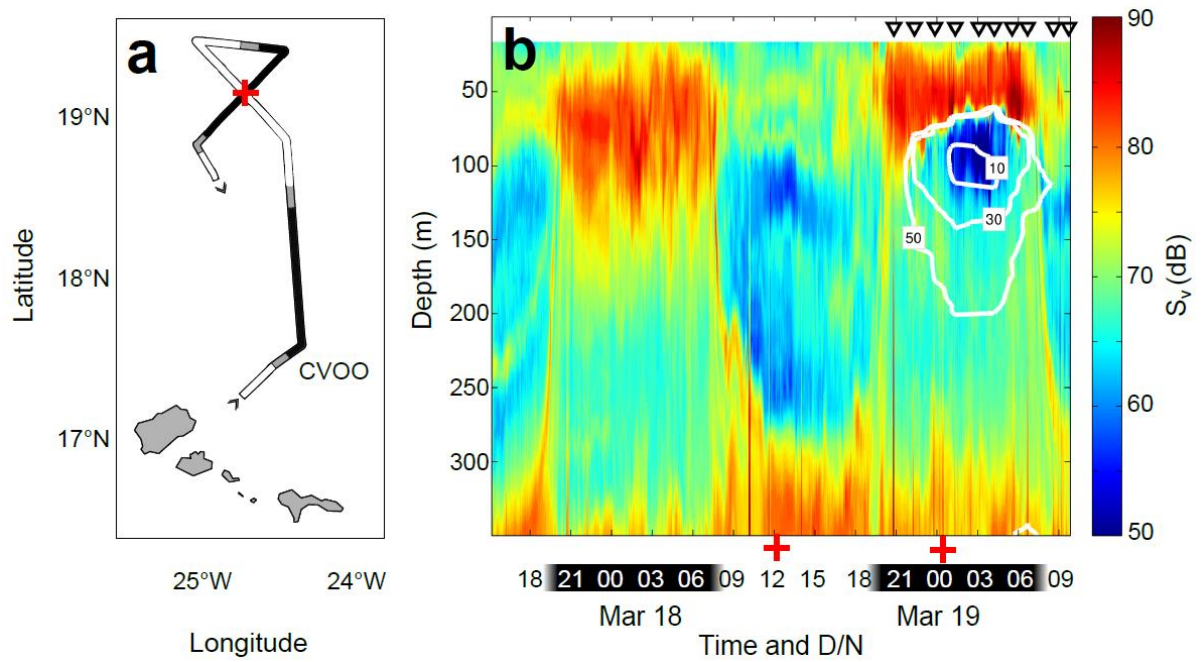
645 **Figures**



646

647 Figure 1. Cruise track (M105, only shown from Mar 17 to Mar 20, 2014) with horizontal
648 current velocities (arrows) and CTD/UVP sampling positions (triangles) as well as multinet
649 stations (gray circles = night, empty circles = day). Large dashed circle indicates the
650 estimated radius of the eddy based upon current structure.

651



652

653 Figure 2. Cruise track with indicated day- and nighttime hours (panel a, red cross indicates
 654 intersection of day- and nighttime section) and Shipboard Acoustic Doppler Current Profiler
 655 (ADCP) mean volume backscatter S_v at 75 kHz (panel b, red crosses indicate the two profiles
 656 obtained at the intersection). White contour lines indicate oxygen concentrations interpolated
 657 from CTD profiles (triangles denote CTD stations).

658

659

660

661

662

663

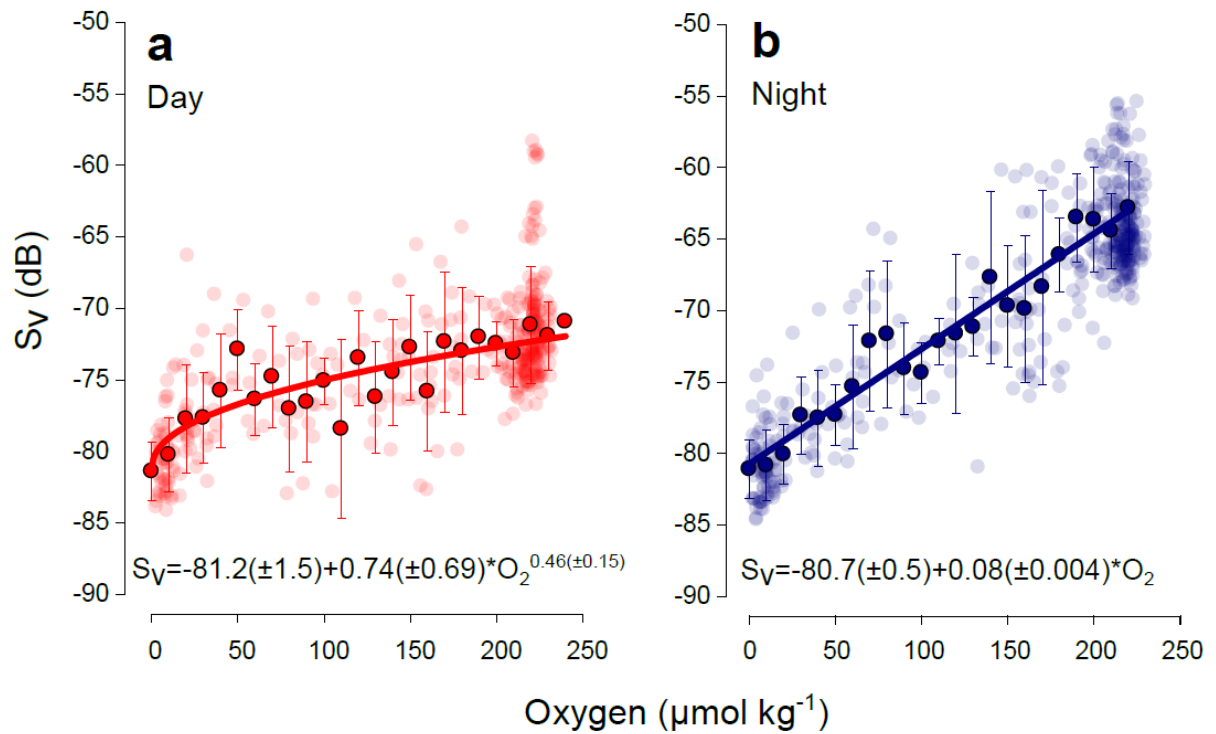
664

665

666

667

668



669

670 Figure 3. Moored ADCP (300 kHz, matched to depth of moored oxygen sensor) mean volume
 671 backscatter S_v (dB) as a function of oxygen concentration ($\mu\text{mol O}_2 \text{ kg}^{-1}$) during daytime (a)
 672 and nighttime hours (b). Higher S_v indicates a higher biomass of zooplankton and nekton.
 673 Transparent symbols are 1.5 hourly data, filled symbols are mean values ($\pm\text{SD}$) for $10 \mu\text{mol}$
 674 $\text{O}_2 \text{ kg}^{-1}$ bins. Data are from Jan 1 to Mar 14, 2010.

675

676

677

678

679

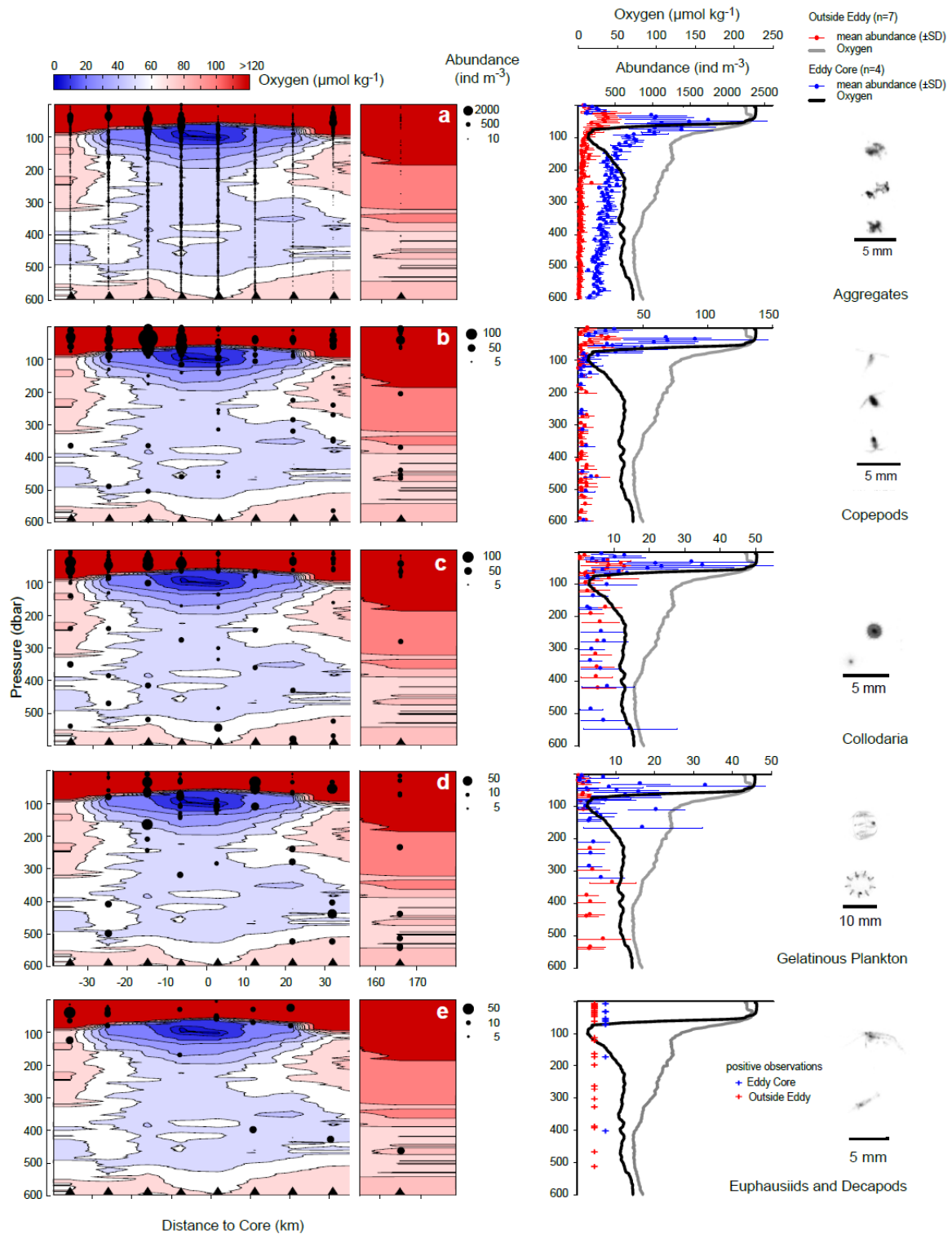
680

681

682

683

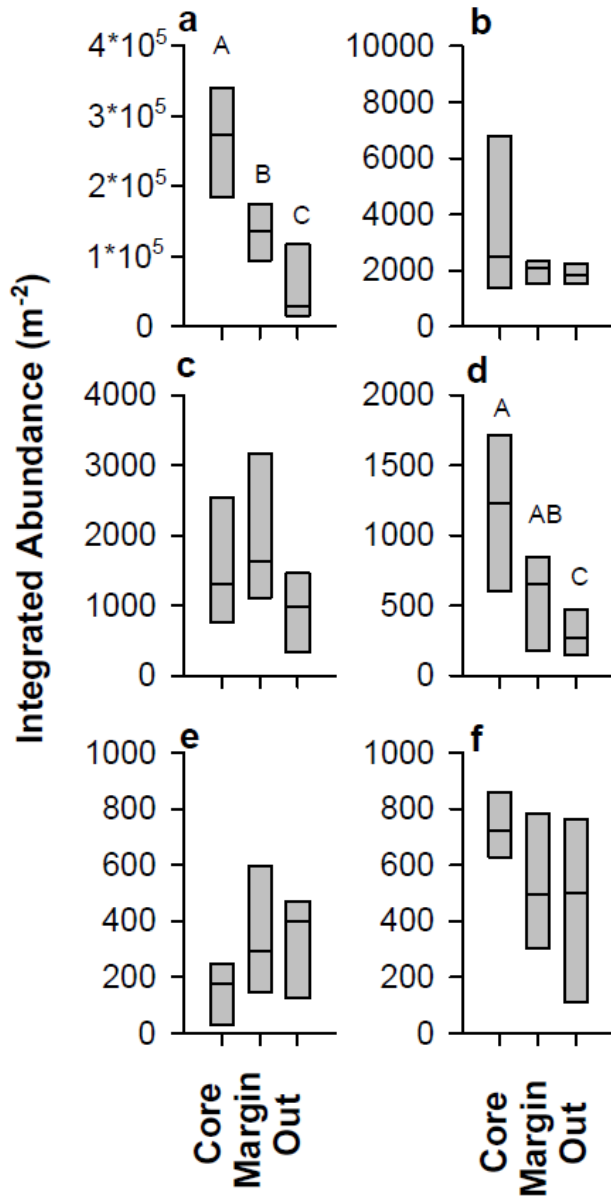
684



685

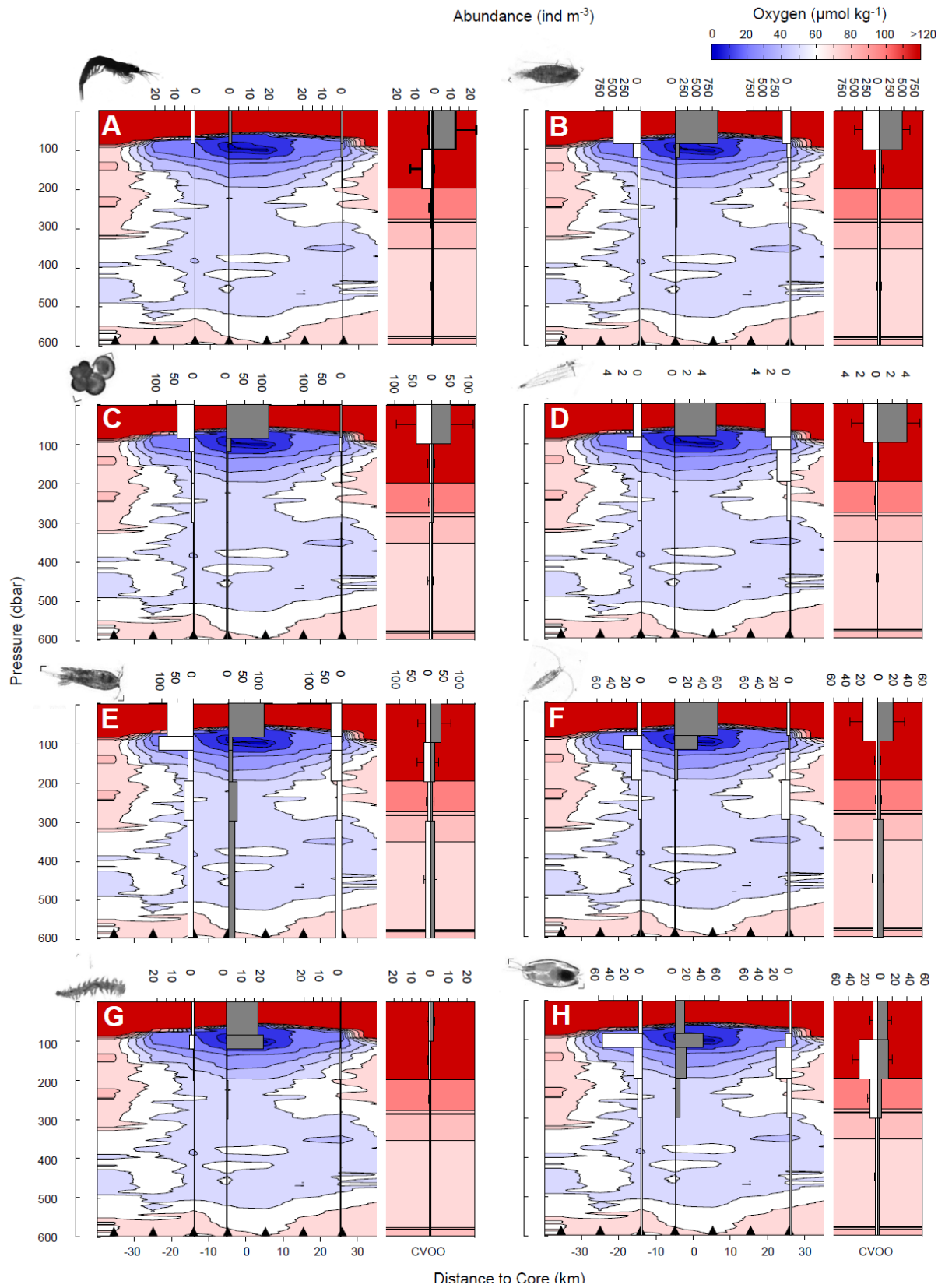
686 Figure 4. Left column shows oxygen contours ($\mu\text{mol O}_2 \text{ kg}^{-1}$) across the eddy (from NE to
 687 SW) with superimposed bubble plots of UVP-based abundance (individuals m^{-3} , in 5 m depth
 688 bins) of aggregates (panel a), copepods (b), collodaria (c), gelatinous plankton (d) and
 689 “shrimp-like” organisms (euphausiids and decapods, e). Note break in distance axis on

690 section panels. Triangles denote CTD/UVP stations. Middle column are profiles of mean
 691 (\pm SD) abundance within the eddy core (n=4) and at the CVOO station (n=7) along with mean
 692 oxygen profiles with the exception of euphausiids and decapods (e), where “+” denotes
 693 positive observations. For better visibility at low values, data with mean abundance = 0 are
 694 omitted. Right column shows representative images of the respective category.



695

696 Figure 5. UVP5-derived integrated abundance (m^{-2} , upper 600 m) of large aggregates (>500
 697 μ m, panel a), copepods (b), collodaria (c), gelatinous plankton (d), shrimp-like micronekton
 698 (euphausiids/decapods, e) and phaeodaria (f) in the eddy core (n=4 profiles), eddy margin
 699 (n=4) and outside of the eddy (n=7). Different letters denote significant differences.



700

701 Figure 6. Oxygen contours ($\mu\text{mol O}_2 \text{ kg}^{-1}$) across the eddy (from NE to SW) with
 702 superimposed bar plots of multinet-based abundance (individuals m^{-3}) of euphausiids (a),

703 calanoid copepods (b), foraminifera (c), siphonophores (d), *Oncaea* sp. (e), eucalanid
704 copepods (f), polychaetes (g), and ostracods (h). White and grey bars indicate daylight and
705 nighttime hauls, respectively. Triangles denote CTD stations used for the O₂ section. For the
706 CVOO station (“outside eddy” situation), the mean (+SD) of four D/N samplings is shown
707 and the distance to core is not calculated because data were combined from different cruises.
708 Representative images are shown next to the respective category panel.